Journal of Mathematical Chemistry Vol. 34, Nos. 3–4, November 2003 (© 2003)

Modelling of amperometric biosensors with rough surface of the enzyme membrane

R. Baronas * and F. Ivanauskas

Faculty of Mathematics and Informatics, Vilnius University, Naugarduko 24, 2600 Vilnius, Lithuania
E-mail: romas.baronas@maf.vu.lt; feliksas.ivanauskas@maf.vu.lt

J. Kulys

Institute of Biochemistry, Mokslininku 12, 2600 Vilnius, Lithuania
E-mail: jkulys@bchi.lt

M. Sapagovas

Institute of Mathematics and Informatics, Akademijos 4, 2600 Vilnius, Lithuania
E-mail: m.sapagovas@ktl.mii.lt

Received 23 June 2003

A two-dimensional-in-space mathematical model of amperometric biosensors has been developed. The model is based on the diffusion equations containing a nonlinear term related to the Michaelis–Menten kinetic of the enzymatic reaction. The model takes into consideration two types of roughness of the upper surface (bulk solution/membrane interface) of the enzyme membrane, immobilised onto an electrode. Using digital simulation, the influence of the geometry of the roughness on the biosensor response was investigated. Digital simulation was carried out using the finite-difference technique.

KEY WORDS: reaction–diffusion, modelling, biosensor, rough surface

AMS subject classification: 35K57, 65M06, 76R50, 92C45

1. Introduction

Biosensors are analytical devices in which immobilised biologically active compounds are used in combination with a signal transducer and an electronic amplifier [1–3]. Starting from the publication of Clark and Lyons in 1962 [4], the amperometric biosensors became one of the popular and perspective trends of biosensorics. The amperometric biosensors measure the faradaic current that arises on a working indicator electrode by direct electrochemical oxidation or reduction of the products of the biochemical reaction [5–7]. In amperometric biosensors the potential at the electrode is

* Corresponding author.

held constant while the current is measured. The amperometric biosensors are known to be reliable, cheap and highly sensitive for environment, clinical and industrial purposes [2,3,5,6].

Since it is not generally possible to measure the concentration of substrate inside enzyme membranes with analytical devices, starting form seventies various mathematical models of amperometric biosensors have been developed and used as an important tool to study and optimise analytical characteristics of actual biosensors [8–12]. The goal of this investigation is to make a model allowing an effective computer simulation of membrane biosensors as well as to investigate the influence of the geometrical and kinetic parameters of the biosensors on the response. The developed model is based on non-stationary diffusion equations [13], containing a nonlinear term related to the Michaelis–Menten kinetic of the enzymatic reaction.

The thickness of the enzyme membrane has a considerable effect on the biosensor current as well as response time [2,3,14,15]. Due to the technology of the biosensors preparation it is difficult to ensure absolutely flat surface of the membrane at the bulk solution/membrane interface. This paper deals with the influence of roughness of the upper surface of the enzyme membrane on the biosensor response. Using digital simulation, the influence of the geometry of the roughness on the biosensor response was investigated at wide range of the maximal enzymatic rates and substrate concentrations. The basic thickness of the enzyme membrane was also changed.

In this investigation, the digital simulation of the biosensor response was carried out using the explicit finite difference scheme [16–19]. The program was used for numerical investigation of the kinetics of the biosensors response taking place during phenols detection in waste waters [20].

2. Principal structure of a membrane biosensor

We assume, that the thickness of the enzyme membrane of a biosensor is much less than its length and width. In modelling of roughness of the upper surface (bulk solution/membrane interface) of the enzyme layer, immobilised onto an electrode, we assume that the membrane surface is generally composed of protuberance and underground sites. We investigate two types of the surface roughness.

In a case of the first type of surface roughness, the enzyme layer is modelled by identical longitudinal slabs, distributed uniformly. Figure 1 shows a biosensor, where protuberances are right quadrangular prisms of base $2b$ by c distributed uniformly so, that the distance between them equals to $2(a - b)$. Due to the uniform distribution of the protuberances, it is reasonable to consider only a unit consisting of a single protuberance together with the basic enzyme layer and an enzyme region between two adjacent protuberances. Because of the symmetry of such unit we may consider only its half. The relatively great length of the unit allows to consider only the transverse section of the half of the unit. Figure 2 shows a profile of the considering unit of the biosensor. The profile parameter a stands for the width of the entire unit, while parameter b stands for

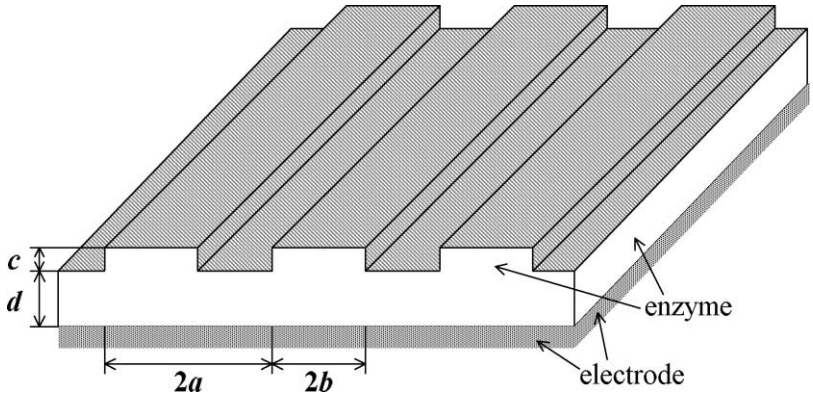

Figure 1. Principal structure of the biosensor when the roughness of the enzyme layer surface is modelled by identical longitudinal slabs, distributed uniformly. The figure is not to scale.

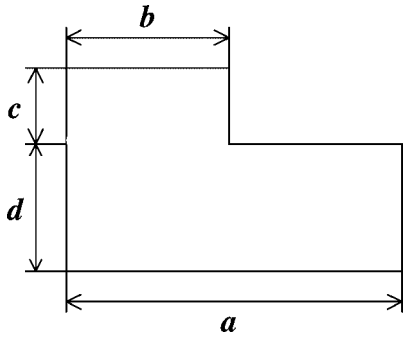

Figure 2. The profile of the biosensor membrane at z plane. d is the basic thickness of the enzyme layer, a is the width of a unit. The protuberance is a rectangle b by c in the transverse section.

the width of the protuberance. The third parameter c is the height of the enzyme layer roughness.

In a case of the second type of the surface roughness, the enzyme membrane is modelled by identical right cylinders, distributed uniformly on the basic enzyme surface. Figure 3 shows a biosensor, where protuberant cylinders of radius b and height c are arranged in a rigid hexagonal array. The distance between centres of two adjacent cylinders equals to $2a$. Due to the uniform distribution of the protuberant cylinders, the entire enzyme layer may be divided into equal hexagonal prisms with regular hexagonal bases. For simplicity, it is reasonable to consider a circle of radius a whose area equals to that of the hexagon and to regard one of the cylinders as a unit cell of the enzyme layer. Due to the symmetry of the unit cell, we may consider only a half of the transverse section of the unit cell. Very similar approach has been used in modelling of partially blocked electrodes [21–23]. Figure 2 shows the profile of the considering unit of the biosensor, presented schematically in figure 3.

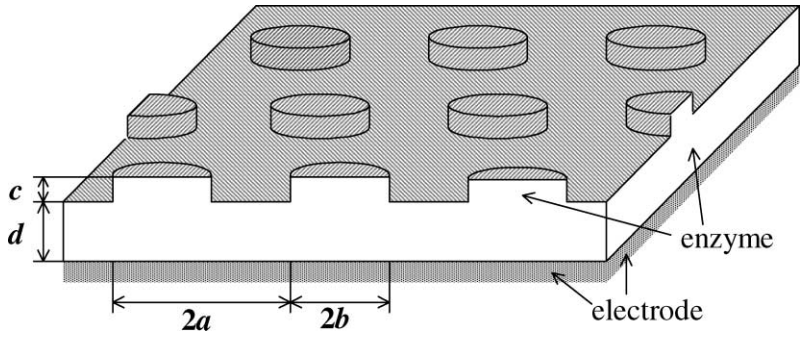

Figure 3. Principal structure of the biosensor when the roughness of the enzyme layer surface is modelled by identical cylinders, distributed uniformly so, that the enzyme layer may be divided into identical hexagonal prisms with regular hexagonal bases. The figure is not to scale.

3. Mathematical model

We consider an enzyme-catalysed reaction when the substrate binds to enzyme and converts to the product.

We have discussed two different types of roughness of the surface of the enzyme membrane. However, the profile at z plane (figure 2) is the same for both types of the roughness. Nevertheless, the corresponding mathematical models have to be formulated differently. In the case, when the biosensor structure looks like the structure presented in figure 1, we formulate two-dimensional-in-space (2-D) model in Cartesian coordinates, while in the next case (figure 3) we formulate 2-D model in cylindrical ones.

3.1. 2-D model in Descartes coordinates

Let Ω_{D} be the closed region, restricted with the concave hexagon, presented in figure 2, Ω_{D}^0 be the corresponding open region, and Γ_{D} – the upper border of that region

$$\Omega_{\mathrm{D}} = \big\{(x,z)\colon\ 0 \leqslant x \leqslant a, 0 \leqslant z \leqslant d\big\} \cup \big\{(x,z)\colon\ 0 \leqslant x \leqslant b, d \leqslant z \leqslant d+c\big\}, \quad (1)$$

$$\Omega_{\mathrm{D}}^0 = \big\{(x,z)\colon\ 0 < x < a, 0 < z < d\big\} \cup \big\{(x,z)\colon\ 0 < x < b, d \leqslant z < d+c\big\}, \quad (2)$$

$$\Gamma = \big\{(x,d+c)\colon\ 0 \leqslant x \leqslant b\big\} \cup \big\{(x,d)\colon\ b \leqslant x \leqslant a\big\} \cup \big\{(b,z)\colon\ d \leqslant z \leqslant d+c\big\}. \quad (3)$$

Considering two-dimensional-in-space diffusion, coupling of enzyme catalysed reaction with the diffusion described by Fick's law, leads to the following equations:

$$\frac{\partial S}{\partial t} = D_{\mathrm{S}}\frac{\partial^2 S}{\partial x^2} + D_{\mathrm{S}}\frac{\partial^2 S}{\partial z^2} - \frac{V_{\max} S}{K_{\mathrm{M}} + S}, \quad (4)$$

$$\frac{\partial P}{\partial t} = D_{\mathrm{P}}\frac{\partial^2 P}{\partial x^2} + D_{\mathrm{P}}\frac{\partial^2 P}{\partial z^2} + \frac{V_{\max} S}{K_{\mathrm{M}} + S}, \quad (x,z) \in \Omega_{\mathrm{D}}^0,\ 0 < t \leqslant T, \quad (5)$$

where $S = S(x,z,t)$ is the substrate concentration, $P = P(x,z,t)$ is concentration of the reaction product, D_{S} and D_{P} are the diffusion coefficients of the substrate and

product, respectively, $V_{\max}$ is the maximal enzymatic rate attainable with that amount of enzyme, when the enzyme is fully saturated with substrate, K_M is the Michaelis constant, t is time, and T is full time of the biosensor operation.

Let $z = 0$ represents the electrode surface, while Γ_D represents the bulk solution/membrane interface. The operation of biosensor starts when some substrate appears over the surface of the enzyme membrane. This is used in the initial conditions ($t = 0$)

$$S(x, z, 0) = 0, \quad (x, z) \in \Omega_D \backslash \Gamma_D, \tag{6}$$

$$S(x, z, 0) = S_0, \quad (x, z) \in \Gamma_D, \tag{7}$$

$$P(x, z, 0) = 0, \quad (x, z) \in \Omega_D, \tag{8}$$

where S_0 is the concentration of substrate (bulk) swilling the biosensor.

The following boundary conditions express the symmetry of the unit cell on both sides of the region Ω_D: $x = 0$ and $x = a$ ($0 < t \leqslant T$):

$$\left.\frac{\partial S}{\partial x}\right|_{x=0} = \left.\frac{\partial S}{\partial x}\right|_{x=a} = \left.\frac{\partial P}{\partial x}\right|_{x=0} = \left.\frac{\partial P}{\partial x}\right|_{x=a} = 0. \tag{9}$$

Because of electrode polarisation, the concentration of the reaction product at the electrode surface is being permanently reduced to zero. The substrate does not react at the electrode surface. If the substrate is well-stirred and in powerful motion, then the concentration of substrate as well as product over the enzyme surface (bulk solution/membrane interface, Γ_D) remains constant while the biosensor contacts with the substrate. This is used in the boundary conditions ($0 < t \leqslant T$) given by

$$P(x, 0, t) = 0, \quad 0 \leqslant x \leqslant a, \tag{10}$$

$$\left.\frac{\partial S}{\partial z}\right|_{z=0} = 0, \tag{11}$$

$$S(x, z, t) = S_0, \quad (x, z) \in \Gamma_D, \tag{12}$$

$$P(x, z, t) = 0, \quad (x, z) \in \Gamma_D. \tag{13}$$

The measured current is accepted as a response of a biosensor in a physical experiment. The current depends upon the flux of the reaction product at the electrode surface, i.e., at the border $z = 0$. Consequently, the density $i(t)$ of the current at time t can be obtained explicitly from Faraday's law and Fick's law using the flux of the product concentration P at the surface of the electrode

$$i(t) = n_e F D_P \frac{1}{a} \int_0^a \left.\frac{\partial P}{\partial z}\right|_{z=0} \mathrm{d}x, \tag{14}$$

where n_e is a number of electrons involved in a charge transfer at the electrode surface, and F is Faraday constant, $F = 96485$ C/mol.

3.2. 2-D model in cylindrical coordinates

Since the profile at z plane (figure 2) is the same for both types of the roughness, the domain to be considered in the case of cylindrical coordinates can be expressed by replacing the coordinate x with coordinate r in definitions (1)–(3):

$$\Omega_C = \{(r,z):\ 0 \leqslant r \leqslant a, 0 \leqslant r \leqslant d\} \cup \{(r,z):\ 0 \leqslant r \leqslant b, d \leqslant z \leqslant d+c\}, \quad (15)$$

$$\Omega_C^0 = \{(r,z):\ 0 < r < a, 0 < r < d\} \cup \{(r,z):\ 0 < r < b, d \leqslant z < d+c\}, \quad (16)$$

$$\Gamma_C = \{(r,d+c):\ 0 \leqslant r \leqslant b\} \cup \{(r,d):\ b \leqslant r \leqslant a\} \cup \{(b,z):\ d \leqslant z \leqslant d+c\}. \quad (17)$$

Then the change of the substrate concentration $S = S(r,z,t)$ as well as the reaction product concentration $P = P(r,z,t)$ in the enzyme membrane can be expressed in cylindrical coordinates as follows:

$$\frac{\partial S}{\partial t} = D_S \frac{1}{r}\frac{\partial}{\partial r}\left(r\frac{\partial S}{\partial r}\right) + D_S \frac{\partial^2 S}{\partial z^2} - \frac{V_{max} S}{K_M + S}, \quad (18)$$

$$\frac{\partial P}{\partial t} = D_P \frac{1}{r}\frac{\partial}{\partial r}\left(r\frac{\partial P}{\partial r}\right) + D_P \frac{\partial^2 P}{\partial z^2} + \frac{V_{max} S}{K_M + S}, \quad (r,z) \in \Omega_C^0,\ 0 < t \leqslant T. \quad (19)$$

The initial ($t = 0$) as well as boundary ($0 < t \leqslant T$) conditions in cylindrical coordinates can be formulated similarly to the ones defined in Descartes coordinates

$$S(r,z,0) = 0, \quad (r,z) \in \Omega_C \backslash \Gamma_C, \quad (20)$$

$$S(r,z,0) = S_0, \quad (r,z) \in \Gamma_C, \quad (21)$$

$$P(r,z,0) = 0, \quad (r,z) \in \Omega_C, \quad (22)$$

$$\left.\frac{\partial S}{\partial r}\right|_{r=0} = \left.\frac{\partial S}{\partial r}\right|_{r=a} = \left.\frac{\partial P}{\partial r}\right|_{r=0} = \left.\frac{\partial P}{\partial r}\right|_{r=a} = 0, \quad (23)$$

$$P(r,0,t) = 0, \quad 0 \leqslant r \leqslant a, \quad (24)$$

$$\left.\frac{\partial S}{\partial z}\right|_{z=0} = 0, \quad (25)$$

$$S(r,z,t) = S_0, \quad (26)$$

$$P(r,z,t) = 0, \quad (r,z) \in \Gamma_C,\ 0 < t \leqslant T. \quad (27)$$

The base of the unit cell of the biosensor is a circle of radius a. Because of this the density $i(t)$ of the biosensor current at time t can be calculated as follows:

$$i(t) = n_e F D_P \frac{1}{\pi a^2}\int_0^{2\pi}\int_0^a \left.\frac{\partial P}{\partial z}\right|_{z=0} r\,dr\,d\varphi = n_e F D_P \frac{1}{\pi a^2} 2\pi \int_0^a \left.\frac{\partial P}{\partial z}\right|_{z=0} r\,dr$$
$$= n_e F D_P \frac{2}{a^2}\int_0^a \left.\frac{\partial P}{\partial z}\right|_{z=0} r\,dr, \quad (28)$$

where φ is the third cylindrical coordinate.

4. Digital simulation

Definite problems arise when solving analytically the nonlinear partial differential equations with complex boundary conditions [13,17]. To obtain an approximate analytical solution, approximation and classification of each different condition are needed [14,23]. On the other hand, digital simulation can be applied almost to any case. Consequently, the problem was solved numerically.

The finite difference technique was applied for discretization of the mathematical model [16]. We introduced an uniform discrete grid in all directions: $x(r)$, z and t. An explicit finite difference scheme has been built as a result of the difference approximation of the model. Having a numerical solution of the problem, the density of the biosensor current can be calculated easily.

The explicit scheme has usually a slower processing speed than the implicit one, but is easier to program. The explicit finite difference-based simulator is satisfactory to use because the processing speed of modern computers is high enough to ensure its use is practical. The type of coordinate frame either Descartes or cylindrical is a parameter of the computer program, developed for simulation of the biosensors operation.

The mathematical model as well as the numerical solution of the model was evaluated for different values of the maximal enzymatic rate $V_{\max}$, substrate concentration S_0 and the geometry of the membrane. The following values of the parameters were constant in the numerical simulation of all the experiments:

$$D_{\mathrm{S}} = D_{\mathrm{P}} = 3.0 \cdot 10^{-6}\ \mathrm{cm}^2/\mathrm{s}, \qquad K_{\mathrm{M}} = 1.0 \cdot 10^{-7}\ \mathrm{mol/cm}^3, \qquad n_{\mathrm{e}} = 2. \tag{29}$$

The maximal biosensor current $i_{\max}$ (the biosensor response) as well as the time moment of occurrence of the maximal current (response time) were assumed and analysed as ones of the most important characteristics of biosensors.

In digital simulation, the biosensor response time was assumed as the time when the absolute current slope value falls below a given small value normalised with the current value. In other words, the time

$$T_{\mathrm{R}} = \min_{i(t)>0} \left\{ t\colon \frac{1}{i(t)} \left| \frac{\partial i(t)}{\partial t} \right| < \varepsilon \right\} \tag{30}$$

needed to achieve a given dimensionless decay rate ε is used.

Consequently, the maximal biosensor current $i_{\max}$ was assumed as the current at the biosensor response time T_{R}. We employed $\varepsilon = 10^{-5}$. However, the response time T_{R} as an approximate steady-state time is very sensitive to the decay rate ε, i.e., $T_{\mathrm{R}} \to \infty$, when $\varepsilon \to 0$. Because of this we investigate the change of a half of steady-state time [13]. The resultant relative output signal function $i^*(t)$ can be expressed as:

$$i^*(t) = \frac{i_{\mathrm{R}} - i(t)}{i_{\mathrm{R}}}, \qquad i_{\mathrm{R}} = i(T_{\mathrm{R}}), \qquad i_{\max} = i_{\mathrm{R}}, \tag{31}$$

where $i(t)$ is the output current density at time t as defined in (14) and (28), i_{R} is assumed as the steady-state current i_∞ . Let us notice, that $0 \leqslant i^*(t) \leqslant 1$ at all $t \geqslant 0$, $i^*(0) = 1$

and $i^*(T_R) = 0$. Let $T_{0.5}$ be the time at which the reaction–diffusion process reaches the medium, called half-time of steady-state or, particularly, half of the time moment of occurrence of the maximal current, i.e., $i^*(T_{0.5}) = 0.5$.

5. Results and discussion

Using computer simulation we have investigated the dependence of the maximal biosensor current as well as biosensor response time on the geometry of the membrane surface roughness. The maximal biosensor current i_{max} was assumed as steady-state current i_∞, calculated at the response T_R time defined in (30), $i_{max} = i_\infty = i_R$. The characteristics a, b and c of the enzyme membrane domain Ω_D as well as Ω_C (figure 2) were expressed through the basic thickness d of the enzyme layer

$$a = \alpha d, \qquad b = \beta a = \alpha\beta d, \qquad c = \gamma d. \tag{32}$$

The parameter α expresses the relative width of the single unit (cell) of the biosensor membrane. α characterises also a frequency of the protuberances on the membrane surface. The parameter β stands for the relative width of the protuberances. The third parameter γ stands for the relative height of the enzyme layer roughness. The case when $\gamma = 0$ corresponds to the enzyme membrane having no protuberances on the membrane surface, i.e., the membrane surface is assumed as absolutely flat. Varying these three (α, β and γ) parameters, we model the enzyme layer roughness of the different relative width and height as well as frequency of recurrence of the protuberances. To investigate the effect of the geometry of the membrane surface roughness we have calculated the maximal biosensor response at the following values of α, β and γ:

$$\alpha = 1, 2, 4; \tag{33}$$

$$\beta = 0.25, 0.5, 0.75; \tag{34}$$

$$\gamma = 0, \frac{1}{2N_c}, \frac{2}{2N_c}, \ldots, \frac{N_c}{2N_c}, \quad N_c = 20. \tag{35}$$

Figures 4–6 show results of calculations at given values of the characteristics α, β, γ of the geometry of the membrane surface roughness, maximal enzymatic rate V_{max} of 10^{-7} mol/cm^{3}s, substrate concentration S_0 of $2 \cdot 10^{-8}$ mol/cm^3 and membrane thickness d of 0.01 cm.

Figure 4 presents the dependence of the maximal biosensor current i_{max} on the relative height γ of the enzyme layer protuberances, changing the cell size α, at constant relative width β of 0.5. One can see in figure 4, the maximal biosensor current decreases with increase of relative height γ at all considered values of the cell size α: 1, 2 and 4. This can be explained by the change of the volume of the protuberances. Keeping α and β constant, the volume of the biosensor protuberances increases with increase of height γ. The decrease of i_{max} is especially notable at large values of α. On the other hand, the decrease of i_{max} is more notable in cases, when calculations were carried out in Descartes coordinates than in cylindrical ones.

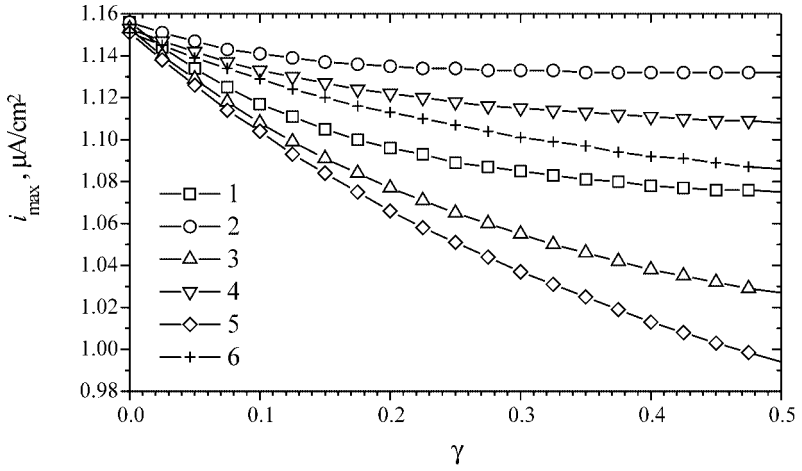

Figure 4. The maximal biosensor current $i_{\max}$ versus the relative height γ of the enzyme layer roughness at different values of the roughness characteristic α: $\alpha = 1$ (1, 2), $\alpha = 2$ (3, 4), $\alpha = 4$ (5, 6), calculated in Descartes (1, 3, 5) and cylindrical (2, 4, 6) coordinates at $\beta = 0.5$, $V_{\max} = 10^{-7}$ mol/cm^{3}s, $S_0 = 2 \cdot 10^{-8}$ mol/cm^{3}s, $d = 0.01$ cm.

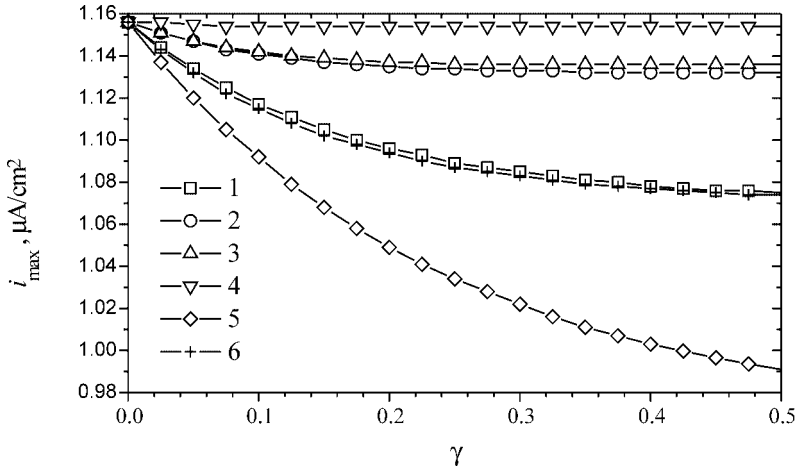

Figure 5. The dependence of the maximal biosensor current $i_{\max}$ on the relative height γ of the enzyme layer roughness at different values of the characteristic β: $\beta = 0.5$ (1, 2), $\beta = 0.25$ (3, 4), $\beta = 0.75$ (5, 6), calculated in Descartes (1, 3, 5) and cylindrical (2, 4, 6) coordinates at $\alpha = 1$, $V_{\max} = 10^{-7}$ mol/cm^{3}s, $S_0 = 2 \cdot 10^{-8}$ mol/cm^{3}s, $d = 0.01$ cm.

Let k_{D} (k_{C}) be the ratio of the volume of all the protuberances to the volume of the entire enzyme domain when the roughness of the enzyme membrane are modelled by Descartes (cylindrical) coordinates

$$k_{\mathrm{D}}(\beta, \gamma) = \frac{bc}{ad + bc} = \frac{\alpha\beta d\gamma d}{\alpha d d + \alpha\beta d\gamma d} = \frac{\beta\gamma}{1 + \beta\gamma}, \tag{36}$$

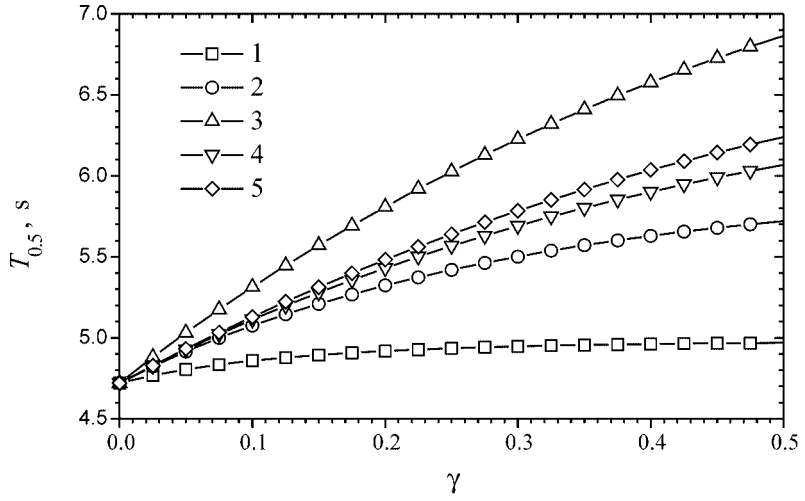

Figure 6. Dependence of the half-time $T_{0.5}$ of the maximal biosensor current on the relative height γ of the enzyme layer roughness at different values of the parameters α: $\alpha = 1$ (1, 2, 3), $\alpha = 2$ (4), $\alpha = 4$ (5) and β: $\beta = 0.25$ (1), $\beta = 0.5$ (2, 4, 5), $\beta = 0.75$ (3), calculated in Descartes coordinates at $V_{\max} = 10^{-7}$ mol/cm^{3}s, $S_0 = 2 \cdot 10^{-8}$ mol/cm^{3}s, $d = 0.01$ cm.

$$k_{\mathrm{C}}(\beta, \gamma) = \frac{\pi b^2 c}{\pi a^2 d + \pi b^2 c} = \frac{(\alpha\beta d)^2 \gamma d}{(\alpha d)^2 d + (\alpha\beta d)^2 \gamma d} = \frac{\beta^2 \gamma}{1 + \beta^2 \gamma}. \tag{37}$$

Ratio k_{D} as well as k_{C} can be called also as a relative volume of the protuberances of the enzyme membrane.

The variation of α, keeping β and γ constant, does not change the volume of the membrane. Since $i_{\max}$ varies with α (figure 4), the biosensor response depends also on the shape of the protuberances not only on their volume.

Figure 5 shows the dependence of the maximal biosensor current $i_{\max}$ on the relative height γ of the membrane protuberances, changing the relative width β, at constant cell size, $\alpha = 1$. According to (36) and (37), the variation of β changes the volume of the membrane. One can see in figure 5, a greater relative width β of the protuberances corresponds to a greater value of the biosensor current $i_{\max}$. However, some pairs of curves are approximately the same. For example, the curve corresponding to $\beta = 0.5$ and Descartes coordinates, is practically identical to an another curve which corresponds to $\beta = 0.75$, calculated in cylindrical coordinates (figure 5). This can be explained by approximate equality of the ratio $k_{\mathrm{D}}(0.5, \gamma)$ and $k_{\mathrm{C}}(0.75, \gamma)$ at all $\gamma \geqslant 0$. Let us notice, that $k_{\mathrm{C}}(\beta, \gamma) = k_{\mathrm{D}}(\beta^2, \gamma)$. Since $k_{\mathrm{D}}(0.25, \gamma) = k_{\mathrm{C}}(0.5, \gamma)$ we can see also an another pair of very similar curves in figure 5. Thus, two biosensors having the same thickness d of the basic enzyme layer, the relative with α of the cell and the relative volume of the protuberances give approximately the same biosensor response.

Figure 6 shows, that the half-time $T_{0.5}$ of the maximal current increases significantly with increase of each of three parameters α, β and γ. For example, in a case of Descartes coordinates when $\alpha = 1$, $\beta = 0.5$ and $\gamma = 0.5$, $T_{0.5}$ is about 1.5 times

greater than in the case of absolutely flat membrane surface, $\gamma = 0$. Figure 6 plots the half-time $T_{0.5}$ obtained from the model, formulated in Descartes coordinates only. In the case of cylindrical coordinates, variation of half-time $T_{0.5}$ is less notable. This can be explained by a relatively less volume of protuberances, $k_C(\beta, \gamma) < k_D(\beta, \gamma)$ at $0 < \beta < 1$, $\gamma > 0$.

The biosensor response considerably depends on the fact either enzyme kinetics or the mass transport predominate in the biosensor response [2,3,15,24,25]. The biosensor response is known to be under control of mass transport if the enzymatic reaction in the enzyme membrane is faster than the transport process. The concentration of substrate reaches zero inside the enzyme layer when the dimensionless diffusion modulus σ^2, Damkoehler number,

$$\sigma^2 = \frac{V_{\max} d^2}{D_S K_M} \tag{38}$$

is much greater than unity.

The diffusion modulus essentially compares the rate of enzyme reaction ($V_{\max}/K_M$) with the diffusion through the enzyme layer (d^2/D_S). If $\sigma^2 < 1$, then enzyme kinetics predominate in the biosensor response. The response is under diffusion control, when the diffusion modulus is greater that unity, $\sigma^2 > 1$, which is observed at high catalytic activity and great membrane thickness or at low Michaelis constant (K_M) or diffusion coefficient (D_S) values.

In the low substrate concentration case, $S_0 \ll K_M$, accepting one-dimensional-in-space model, the stationary biosensor current i_∞ can be calculated from the well-known analytical solution given by Kulys [24]

$$i_\infty = \lim_{t\to\infty} i(t) = n_e F D_S S_0 \frac{1}{d}\left(1 - \frac{1}{\cosh(\sigma)}\right). \tag{39}$$

In the case when $\gamma = 0$ and $S_0 = 0.2K_M < K_M$, we may compare the maximal biosensor $i_{\max} = 1.16\ \mu\text{A/cm}^2$ calculated numerically (figure 4) with the stationary current $i_\infty = 1.15\ \mu\text{A/cm}^2$ calculated by (39). That values compares favourably as it was expected.

Using formula (39) we can find the membrane thickness d, at which the state–state current i_∞ gains the maximum at given n_e, D_S, S_0, $V_{\max}$, K_M and $S_0 \ll K_M$. At first, we calculate a derivative of $i_\infty(d)$ with the respect to the thickness d:

$$\frac{\partial i_\infty(d)}{\partial d} = n_e F D_S S_0 \frac{-\cosh^2(\sigma) + \cosh(\sigma) + \sigma \sinh(\sigma)}{d^2 \cosh^2(\sigma)}. \tag{40}$$

Then we look for σ at which that derivative gets zero:

$$-\cosh^2(\sigma) + \cosh(\sigma) + \sigma \sinh(\sigma) = 0. \tag{41}$$

Equation (41) has been solved numerically. A single solution $\sigma = \sigma_{\max} \approx 1.5055$ was obtained. Consequentially, i_∞ gains the maximum at the membrane thickness $d_{\max}$,

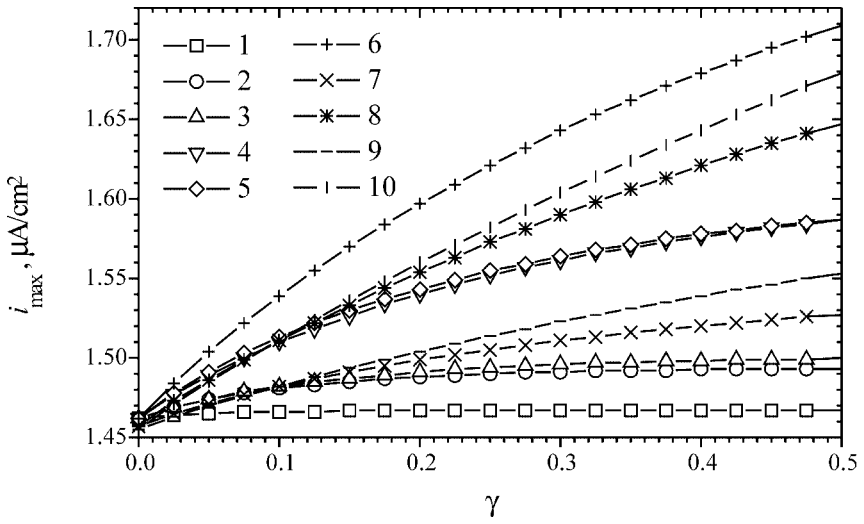

Figure 7. The dependence of the maximal biosensor current $i_{\max}$ on the relative height γ of the enzyme layer roughness at different values of the parameters α and β: $\alpha = 1$ (1–6), $\alpha = 2$ (7, 8), $\alpha = 4$ (9, 10) and $\beta = 0.25$ (1, 2), $\beta = 0.5$ (3, 4, 7–10), $\beta = 0.75$ (5, 6), calculated in Descartes (2, 4, 6, 8, 10) and cylindrical (1, 3, 5, 7, 9) coordinates at $V_{\max} = 10^{-7}$ mol/cm^{3}s, $S_0 = 2 \cdot 10^{-8}$ mol/cm^{3}s, $d = 0.001$ cm.

where

$$d_{\max} = \frac{1}{\sigma_{\max}} \sqrt{\frac{D_S K_M}{V_{\max}}}, \quad \sigma_{\max} = 1.5055. \tag{42}$$

Accepting (29), we find, that $d_{\max} \approx 0.00261$ cm, $i_{\max} \approx 2.56$ μA/cm^2 at $V_{\max} = 10^{-7}$ mol/cm^{3}s. So, the decrease of the maximal current $i_{\max}$ with increase of the roughness height (figure 4) can be explained by the membrane thickness $d = 0.01 > d_{\max}$.

Since the biosensor response considerably depends on the diffusion modulus, we repeat the calculations above with a membrane thickness considerably less than $d_{\max}$, i.e., at which the diffusion modulus σ is less than $\sigma_{\max} = 1.5055$. Accepting (29) and $V_{\max} = 10^{-7}$ mol/cm^{3}s we model the enzyme membrane ten times thinner as before, $d = 0.001$ cm, when $\sigma = 0.577 < \sigma_{\max}$. Consequentially, the diffusion modulus σ^2 equals to 0.33 at $d = 0.001$, while $\sigma^2 = 33.3$ at $d = 0.01$ cm. Thus the biosensor response is under diffusion control in the case of $d = 0.01$, while the enzyme kinetics predominate in the case of $d = 0.001$ cm.

Results of calculations in the case of $d = 0.001$ cm are depicted in figure 7. One can see in figure 7, the maximal biosensor current $i_{\max}$ increases even up to about 17%, while in the case of $d = 0.01$ cm $i_{\max}$ decreases up to about 15% (figures 4, 5). When $d = 0.001$ cm, the maximal current $i_{\max}$ increases with increase of each of three parameters α, β and γ. Figure 7 shows, that two biosensors, satisfying $k_D \approx k_C$, generates approximately the same response as it was noticed in the previous case when $d = 0.01$ cm (figure 5).

One can see (figure 7) the maximal biosensor $i_{\max}$, calculated numerically at $\gamma = 0$, equals to about 1.46 μA/cm^2. The stationary current i_∞, calculated from (39), equals to about 1.69 μA/cm^2. That values differs by about 15%, while the corresponding difference in the case of thicker enzyme membrane, $d = 0.01$, was only about 1%. The formula (39) is applicable in the case of low substrate concentration, $S_0 \ll K_{\mathrm{M}}$. Our calculations were carried out at $S_0 = 0.2K_{\mathrm{M}}$. So, in the case when the reaction rate controls the biosensor response, $\sigma^2 < 1$, the condition $S_0 \ll K_{\mathrm{M}}$ should be especially strictly taken into consideration to calculate the accurate value of the stationary current by (39).

The maximal biosensor current is sensitive to changes of the maximal enzymatic rate $V_{\max}$ and substrate concentration S_0 [2,3,14,15,25]. Changing values of these two parameters, the maximal current varies even in orders of magnitude. Because of this, we investigate the influence of the geometry of the roughness of the membrane surface on the biosensor response at different values of $V_{\max}$ and S_0. Due to the sensitivity of the biosensor response to changes of $V_{\max}$ and S_0, we normalise the maximal biosensor current to evaluate the effect of the geometry of the membrane surface roughness on the biosensor response. Let $i_{\max}(\gamma)$ be the maximal current of a biosensor, having the relative height γ of the enzyme layer roughness. Thus $i_{\max}(0)$ corresponds to the maximal current of a biosensor, having no roughness on the membrane surface. We express the normalised maximal biosensor current i_{Nmax} as the maximal current of the biosensor, having membrane surface roughness, divided by the maximal current of the corresponding biosensor, having no membrane surface roughness,

$$i_{\mathrm{Nmax}}(\gamma) = \frac{i_{\max}(\gamma)}{i_{\max}(0)}. \tag{43}$$

Assuming $T_{0.5}(\gamma)$ as the half-time of the maximal biosensor response at given γ, we introduce normalised half-time $T_{\mathrm{N},0.5}$ as follows:

$$T_{\mathrm{N},0.5}(\gamma) = \frac{T_{0.5}(\gamma)}{T_{0.5}(0)}. \tag{44}$$

Results of calculations at two values of $V_{\max}$: 10^{-7}, 10^{-8} mol/cm^{3}s as well as two values of S_0: $2.0 \cdot 10^{-8}$, $2.0 \cdot 10^{-9}$ mol/cm^{3}s are depicted in figures 8, 9 ($d = 0.01$ cm) and figure 10 ($d = 0.001$ cm). One can see in these figures, the tenfold reducing of $V_{\max}$ influence a significant change of maximal current $i_{\max}$ as well as half-time $T_{0.5}$, while the tenfold reducing of S_0 has no practical influence on $i_{\max}$ as well as $T_{0.5}$. This is noticed in both cases of the membrane thickness d: 0.01 and 0.001 cm.

In the case of the low enzymatic rate, $V_{\max} = 10^{-8}$ mol/cm^{3}s, and thick enzyme membrane, $d = 0.01$ cm, a slight non-monotony of the maximal biosensor current can be noticed (figure 8). In this case the diffusion modulus σ^2 equals to about 3.33, $\sigma \approx 1.84$. That value of σ is rather near to $\sigma_{\max}$, defined in (42). Let us remind, that in the case of 1-D enzyme membrane the stationary current i_∞ is a monotonous increasing function of the thickness at $\sigma < \sigma_{\max}$, while i_∞ monotonous decreases at $\sigma < \sigma_{\max}$.

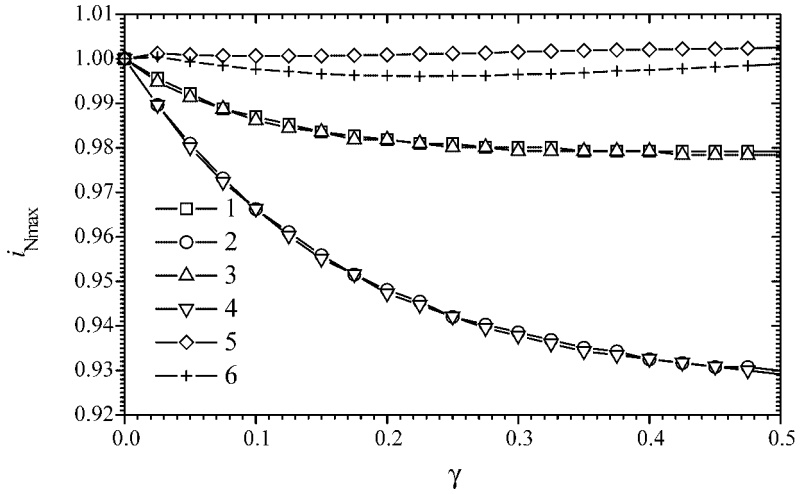

Figure 8. The normalised maximal biosensor current i_{Nmax} versus roughness characteristic γ at different the maximal enzymatic rates $V_{\max}$: $V_{\max} = 10^{-7}$ (1–4), $V_{\max} = 10^{-8}$ (5, 6) mol/cm^{3}s, substrate concentration S_0: $S_0 = 2 \cdot 10^{-8}$ (1, 2, 5, 6), $S_0 = 2 \cdot 10^{-9}$ (3, 4) mol/cm^{3}s, calculated in Descartes (2, 4, 6) and cylindrical (1, 3, 5) coordinates at $\alpha = 1$, $\beta = 0.5$, $d = 0.01$ cm.

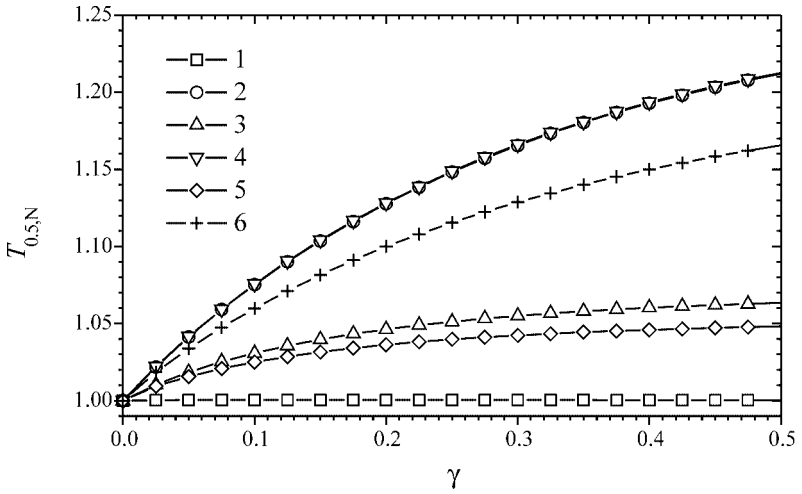

Figure 9. The normalised half-time $T_{\mathrm{N},0.5}$ of the maximal biosensor response versus the roughness characteristic γ. Notation and all parameters are the same as in figure 8.

6. Conclusions

The two-dimensional-in-space mathematical model (4)–(13) of amperometric biosensor operation can be successfully used to investigate the kinetic peculiarities of membrane-based biosensors, having rough surface of the enzyme layer, when the roughness is modelled by identical longitudinal slabs, distributed uniformly (figure 1). Correspondingly, the model (18)–(27) can be used in the case when the roughness is modelled

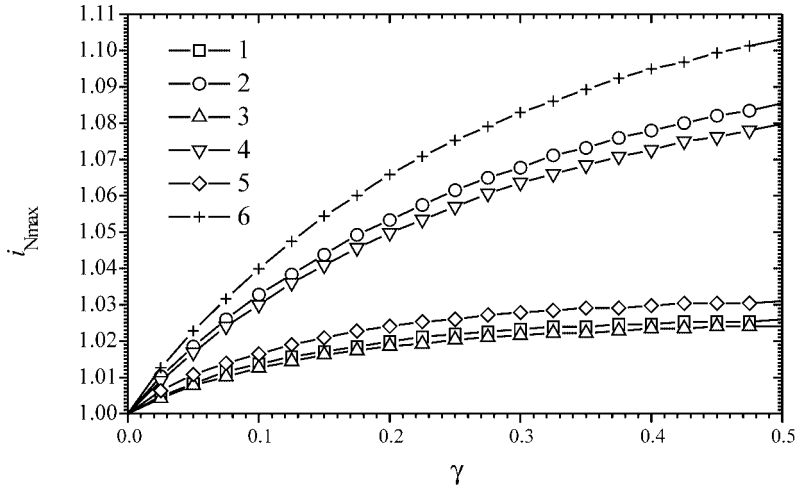

Figure 10. The normalised maximal biosensor current i_{Nmax} versus characteristic γ of the enzyme layer at the membrane thickness $d = 0.001$ cm. Other parameters and notation are the same as in figure 8.

by identical cylinders, arranged in a rigid hexagonal array (figure 2).

The maximal biosensor current $i_{\max}$ decreases with increase of the relative height γ of the protuberances (figures 4, 5 and 8) when the biosensor response is under diffusion control and $i_{\max}$ increases with increase of γ (figures 7, 10) when the enzyme kinetics predominate in the biosensor response. The half-time $T_{0.5}$ of the maximal current always increases with increase of γ (figures 6, 9). The influence of the surface roughness on the biosensor response is more significant at a thinner membrane than at a thicker one.

Two biosensors, having the same basic thickness d of the basic enzyme layer, the relative width α of the cell and the same ratio of the volume of the protuberances to the volume of the entire enzyme membrane, give approximately the same biosensor response (figures 5, 8, 9).

The influence of the roughness of the membrane surface on the biosensor response is more significant at the higher maximal enzymatic rate than at lower one. The ten-fold change of substrate concentration practically does not effects the influence of the roughness of the membrane surface on the biosensor response (figures 8, 10).

Acknowledgements

This work was partially supported by European Commission funded RTD project, contract No. QLK3-CT-2000-01481.

References

[1] G.G. Guilbault, *Analytical Uses of Immobilized Enzymes* (Marcel Dekker, New York, 1984).
[2] A.P.F. Turner, I. Karube and G.S. Wilson, *Biosensors: Fundamentals and Applications* (Oxford University Press, Oxford, 1987).

[3] F. Scheller and F. Schubert, *Biosensors* (Elsevier, Amsterdam, 1992).
[4] L.C. Clarc and C. Loys, Ann. N.Y. Acad. Sci. 102 (1962) 29.
[5] K.R. Rogers, Biosens. Bioelectron. 10 (1995) 533.
[6] U. Wollenberger, F. Lisdat and F.W. Scheller, *Frontiers in Biosensorics 2: Practical Applications* (Birkhäuser, Basel, 1997).
[7] A. Chaubey and B.D. Malhotra, Biosens. Bioelectron. 17 (2002) 441.
[8] G.G. Guilbault and G. Nagy, Anal. Chem. 45 (1973) 417.
[9] C.D. Mell and J.T. Maloy, Anal. Chem. 47 (1975) 299.
[10] C.D. Mell and J.T. Maloy, Anal. Chem. 48 (1976) 1597.
[11] J.J. Kulys, V.V. Sorochinski and R.A. Vidziunaite, Biosensors 2 (1986) 135.
[12] T. Schulmeister, J. Rose and F. Scheller, Biosens. Bioelectron. 12 (1997) 1021.
[13] J. Crank, *The Mathematics of Diffusion*, 2nd ed. (Clarendon Press, Oxford, 1975).
[14] T. Schulmeister, Selective Electrode Rev. 12 (1990) 203.
[15] R. Baronas, F. Ivanauskas and J. Kulys, Nonlinear Analysis: Modelling and Control 8 (2003) 3.
[16] W.F. Ames, *Numerical Methods for Partial Differential Equations*, 2nd ed. (Academic Press, New York, 1977).
[17] D. Britz, *Digital Simulation in Electrochemistry*, 2nd ed. (Springer, Berlin, 1988).
[18] P.N. Bartlett and K.F.E. Pratt, Biosens. Bioelectron. 8 (1993) 451.
[19] K. Yokoyama and Y. Kayanuma, Anal. Chem. 70 (1998) 3368.
[20] EC RTD Project. INTELLISENS: Intelligent Signal Processing of Biosensor Arrays Using Pattern Recognition for Characterisation of Wastewater: Aiming Towards Alarm Systems, 2000–2003.
[21] T. Gueshi, K. Tokuda and H. Matsuda, J. Electroanal. Chem. 89 (1978) 247.
[22] C. Deslous, C. Gabrielli, M. Keddam, A. Khalil, R. Rosset, B. Trobollet and M. Zidoune, Electrochim. Acta 42 (1997) 1219.
[23] R. Baronas, F. Ivanauskas and A. Survila, J. Math. Chem. 27 (2000) 267.
[24] J. Kulys, Enzyme Microbiol. Technol. 3 (1981) 344.
[25] R. Baronas, F. Ivanauskas and J. Kulys, J. Math. Chem. 32 (2002) 225.